

# Nonlinear Model Predictive Control for Improving Energy Recovery for Electric Vehicles during Regenerative Braking

Xiaoyu Huang and Junmin Wang\*

Department of Mechanical and Aerospace Engineering  
Ohio State University, Columbus, OH 43210

**Abstract**—This paper presents a nonlinear model predictive control (NMPC) scheme and a case study for improving the regenerative braking (RB) energy recovery for electric vehicles (EV) with in-wheel motors. The first part deals with a braking torque split problem, that is, given a desired vehicle longitudinal velocity profile, design braking torques for front and rear wheels independently to increase the RB energy recovery. The second part provides a case study to see the effects of different vehicle velocity profiles, with the same initial and terminal velocities and desired travelling distance, on RB energy recovery. The controller developed in the first part employs a three degrees-of-freedom longitudinal vehicle dynamic model with explicit considerations on the experimentally-measured, motor-to-battery RB efficiency map. Simulation results show that the proposed NMPC is capable of restoring more RB energy than a conventional PI controller does. The case study clearly shows the great potential in planning *a priori* velocity trajectory that is optimal in terms of energy recovery for RB control of EVs with in-wheel motors.

## I. INTRODUCTION

RECENTLY, emerging electric vehicle technologies show great potentials in relieving the energy consumption concerns in the transportation sector. One significant feature of EVs is the ability of converting/harvesting vehicle kinetic energy into electric energy through regenerative braking (RB) [1]. This recovered energy can in turn be used to power EV in the driving maneuver, thus reducing total energy consumption. As early as 40 years ago, authors in [2] proposed an energy control method for a motor driven vehicle, which allowed RB, with a maximum principle. Recently, some simple and effective RB control strategies were also provided in [3]~[5], where regenerative braking was considered together with the traditional mechanical braking system, and optimum braking force distribution curve was taken into account for stability concerns. Moreover, some other novel controllers were provided in the literature. Cao *et al.* in [6] designed a neural network self-adaptive PID controller, and in [7] combined neural network control with sliding mode control such that stronger robustness was achieved. Zhang *et al.* [8] proposed a fuzzy logic based controller and showed its ability of restoring more energy as well as ensuring braking safety and battery life. Xie *et al.* [9] provided a robust controller based on switched system theory with the main concern of stability during RB.

\*Corresponding author. This research was partially supported by the Office of Naval Research Young Investigator Program (ONR-YIP) Award under Grant N00014-09-1-1018, Honda-OSU Partnership Program, and OSU Transportation Research Endowment Program.

Though successful in restoring RB energy to some extent and dealing with stability problems, previous research seldom treated the following control problems together with energy concerns: track desired vehicle longitudinal velocity profile; and travel desired distance with given initial and terminal velocities. Solutions to the former problem have applications in autonomous/unmanned vehicle controls where the velocity trajectories may be predefined. While solutions to the latter one can be applied to commonly encountered maneuvers on regular vehicles such as deceleration/stop before a red traffic light [10] or transitional maneuvers in adaptive cruise control (ACC) [11]. Furthermore, the motor-to-battery efficiency of regenerative braking [12] is not explicitly considered in any of the previous research. As a matter of fact, with the presence of additional objectives as well as limitations, tradeoffs become possible between control performance and improving RB energy recovery. Nonlinear model predictive control (NMPC) is capable of dealing with complex optimization problems as well as handling some kinds of nonlinearities and constraints, and has been applied in automotive research [13]~[16]. In this paper, an NMPC approach is adopted to address the first problem of velocity tracking for improving RB energy recovery, and a case study illustrating great potentials in significantly increasing RB efficiency by smart design of the velocity profile during deceleration is also provided.

In this study, only the straight-line braking maneuver is considered and it is assumed that no mechanical friction brake is involved. The main objectives of this paper are: first, develop a NMPC to achieve improvement of regenerative braking energy recovery when tracking desired vehicle velocity profile; and second, give insight into the effects that different velocity profiles under the given initial and terminal velocities and total distance can have on RB energy recovery. In the first problem, the front and the rear RB torques are seen as two independent control inputs, while in the second one, only total braking torque is considered as the manipulated input for simplicity, and some techniques that are not introduced may be needed to satisfy multiple terminal constraints. In the design of the NMPC, an experimentally-determined motor-to-battery RB efficiency and constraints on braking torques are explicitly reflected in the NMPC formulations. The main contribution of this paper lies in that it provides the great potential and possibilities of using NMPC to solve multi-objective optimization problems for regenerative braking of electric vehicles.

The rest of this paper is organized as follows: In Section II,

regenerative braking system is introduced. Section III addresses the first problem of velocity profile tracking. Section IV presents the case study for different velocity profiles during deceleration. Simulation results of the proposed NMPC-based RB controller as well as case study are given in Section V, followed by conclusion remarks in Section VI.

## II. ELECTRIC VEHICLE REGENERATIVE BRAKING SYSTEM

For electric ground vehicles (EGV) with in-wheel motors, the regenerative braking system for each wheel can work alone or together with a mechanical friction braking system. In this paper, only braking torques generated by in-wheel motors are in effect. For the cases where RB itself is not sufficient, some cooperative control of mechanical / regenerative braking is needed, yet falls beyond the interest of this paper.

For control purposes, the motor-to-battery efficiency is introduced, as defined below:

$$\eta = \frac{U_c I_c}{T_b \omega}, \quad (1)$$

where,  $U_c$  and  $I_c$  are the measurable battery charging voltage and current during RB, respectively,  $T_b$  is in-wheel motor braking torque, and  $\omega$  is wheel/motor angular speed. It should be noted that the braking torque has excluded the resistance torque (which can be calibrated) embedded in the wheel/motor set, i.e.,  $T_b$  is the net braking torque on an individual wheel.

The regenerative braking efficiency map is generated from EGV chassis dynamometer test under different exerted braking torque values and various wheel speeds. Since battery charging voltage and current can also be measured under given braking torque and wheel speed, the RB efficiency is seen to be a function of braking torque and wheel speed and rewritten in the following form

$$\eta = \eta(T_b, \omega). \quad (2)$$

In order for NMPC design, the efficiency map (as shown in Fig. 1) was fitted using surface fitting tool to be a polynomial of  $T_b$  and  $\omega$  of fourth-order, based on the experimental data obtained on a prototyping EGV with in-wheel motors developed by the Vehicle Systems and Control Laboratory (VSCL) at The Ohio State University. The main features of the in-wheel motor and batteries have been described in [12].

As can be seen from Fig. 1, the efficiency map is not strictly concave or convex. At a given wheel speed, RB efficiency generally has a maximum value under a relatively large braking torque. Moreover, RB can only be triggered when motor speed is higher than 200rpm. This is mainly due to the feature of in-wheel motor and its driver, and will be considered as a constraint in the controller design.

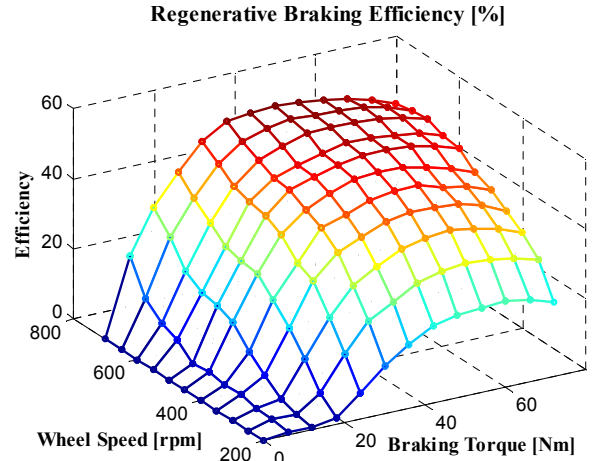


Fig. 1. Regenerative Braking Efficiency Map.

## III. NMPC DESIGN FOR VELOCITY TRACKING

In this problem, the desired vehicle velocity profile is known in advance. The objectives are: 1) to improve RB energy during the whole process; and 2) to track desired velocity as closely as possible. The problem is worthwhile for some applications such as in braking control of autonomous vehicles or wheeled robots, for which velocity trajectories are known *a priori*. A 3-DOFs (degrees-of-freedom) vehicle longitudinal model including wheel dynamics is first described. The reason for inclusion of such a dynamic model is to incorporate constraints brought by longitudinal tire normal load transfer into the NMPC formulation. The problem is more like a control allocation problem with the purpose of optimization and tracking [20].

### A. 3-DOF Longitudinal Vehicle Dynamic Model

The 3-DOFs longitudinal vehicle dynamic model takes vehicle longitudinal velocity  $v$ , front wheel angular speed  $\omega_{wF}$  and rear wheel angular speed  $\omega_{wR}$  as state variables. The individual wheel dynamics are shown in Fig. 2. Note that the actual value of  $F_x$  will be negative during braking.

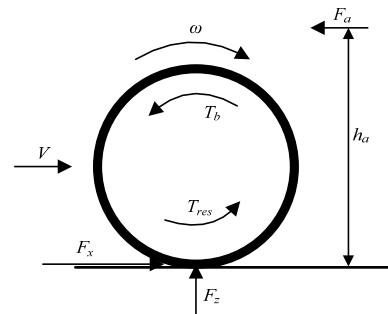


Fig. 2. Individual Wheel Dynamics

The dynamic equations are shown below.

$$m\dot{v} = F_x - F_a = k_x s_F \cdot F_{zF} + k_x s_R \cdot F_{zR} - F_a, \quad (3)$$

$$J \dot{\omega}_{wF} = -T_{bF} - r_e (k_x s_F + \gamma) \cdot F_{zF}, \quad (4)$$

$$J \dot{\omega}_{wR} = -T_{bR} - r_e (k_x s_R + \gamma) \cdot F_{zR}, \quad (5)$$

where  $F_x$ ,  $F_a$ ,  $F_{zF}$  and  $F_{zR}$  are exerted longitudinal tire

force, aerodynamic drag force, front and rear tire normal forces, respectively;  $J$  is the inertia of wheel/motor set,  $m$  is the total mass of vehicle,  $\gamma$  denotes the rolling resistance coefficient,  $r_e$  is the effective radius of tire. Besides,  $s_F$  and  $s_R$  are slip ratios of front and rear wheels, respectively, and  $k_x$  denotes the slip-slope when the slip ratio is under a certain threshold value. For a specific road condition,  $k_x$  is assumed to depend only on tire properties and can be estimated using typical estimation methods such as recursive least-squares (RLS) [18][21]. In this paper, it is satisfied by the constraints on system states and inputs that the tires are always working in the linear region. This constraint also stems from the vehicle safety consideration, that is, tires should work far from the saturation region on the tire characteristic curve. Other details can be found in the NMPC formulation. System inputs are front and rear braking torques,  $T_{bF}$  and  $T_{bR}$ , which should be distributed equally between the left and right wheels due to the negligence of vehicle lateral dynamics.

### B. NMPC Formulation

The proposed NMPC scheme works as follows: at each sampling instant, given the current state as initial state, the optimization problem is solved for designed cost function within a finite time window, and the first element in the solution sequence is applied to the plant. Then, for the next instant, the same procedure is repeated to generate the next control input vector [17].

The NMPC problem can be formulated as below.

#### 1) Model:

The model (3)~(5) after discretization and rearrangement is shown as follows.

$$v(k+1) = \frac{\Delta t}{m} \left[ \begin{array}{l} k_x s_F(k) \cdot F_{zF}(k) \\ + k_x s_R(k) \cdot F_{zR}(k) - F_a(v(k)) \end{array} \right] + v(k), \quad (6)$$

$$\omega_{wF}(k+1) = \frac{\Delta t}{J} \left\{ \begin{array}{l} -T_{bF}(k) \\ -r_e [k_x s_F(k) + \gamma] F_{zF}(k) \end{array} \right\} + \omega_{wF}(k), \quad (7)$$

$$\omega_{wR}(k+1) = \frac{\Delta t}{J} \left\{ \begin{array}{l} -T_{bR}(k) \\ -r_e [k_x s_R(k) + \gamma] F_{zR}(k) \end{array} \right\} + \omega_{wR}(k), \quad (8)$$

where, the input vector is  $\mathbf{u}(k) = [T_{bF}(k) \ T_{bR}(k)]^T$ . The following equations are part of the computation.

$$F_a(v(k)) = C_a v(k)^2, \quad (9)$$

$$F_{zF}(k) = m(l_R g - h \dot{v}(k)) / l - F_a h_a / l, \quad (10)$$

$$F_{zR}(k) = m(l_F g + h \dot{v}(k)) / l + F_a h_a / l, \quad (11)$$

$$s_F(k) = \omega_{wF}(k) r_e / v(k) - 1, \quad (12)$$

$$s_R(k) = \omega_{wR}(k) r_e / v(k) - 1, \quad (13)$$

where,  $C_a$  is the air resistance coefficient,  $l_F$  and  $l_R$  are distances from front axle and rear axle to the EGV center of gravity (c.g.), respectively,  $l$  is the wheelbase,  $h$  is c.g.

height above ground,  $h_a$  is equivalent height of exerting point of aerodynamic drag force.

Note that in the calculation of normal force  $F_{z_i}$ ,  $\dot{v}(k) = [v(k) - v(k-1)] / \Delta t$ , such that the undesirable algebraic loop in the continuous time is avoided.

#### 2) Cost Function:

Considering the two objectives, intuitively, the cost function can be designed to be in the form of (14).

$$J = \min_{\substack{\mathbf{u}(k|k), \dots, \\ \mathbf{u}(k+h_c-1|k)}} \left\{ \begin{array}{l} w_r \left\{ \frac{\sum_{i=1}^{h_p} [y(k+i|k) - y_d(k+i|k)]^2}{\sum_{i=0}^{h_c-1} [\eta(k+i|k)]} \right\} \\ + w_u \sum_{i=1}^{h_c-1} \left\{ \|\mathbf{u}(k+i|k) - \mathbf{u}(k+i-1|k)\|^2 \right\} \end{array} \right\}, \quad (14)$$

$$\eta = \frac{T_{bF} \omega_{wF} \eta_F + T_{bR} \omega_{wR} \eta_R}{T_{bF} \omega_{wF} + T_{bR} \omega_{wR}} \quad (15)$$

where,  $\eta$  is the overall RB efficiencies;  $h_p$  and  $h_c$  are prediction horizon and control horizon;  $w_r$  and  $w_u$  are weighting matrices to determine relative importance of the penalized terms: tracking error and RB efficiency, and braking torque changing rate.

*Remark 1:* Throughout this paper, it is always RB efficiency being penalized in the cost function instead of RB power. This is due to the fact that maximal RB power is not equivalent to highest energy-efficiency. Since the duration time of RB is undetermined, higher RB power at each instant cannot guarantee more energy recovered during the whole RB process.

#### 3) Constraints:

Due to the motor limitation, the highest value of regenerative braking torque for an individual wheel is no more than 80 Nm. From modeling point of view, slip ratio of each wheel should be kept under 0.03 [19] for tires to work in the linear range. From stability point of view, since wheel dynamics are much faster than vehicle body dynamics, to avoid high slip ratio, or in some extreme cases, wheel lock [3]~[5], the maximal braking torque must be adjusted automatically according to the normal load for each wheel. As to normal load, during braking maneuver, the load transfer from rear wheels to front wheels should be taken into account. Therefore, constraints on system inputs and states can be expressed as follows.

$$0 \leq T_{bi} \leq 2T_{b,\max}, \quad (16)$$

$$\omega_{\min} \leq \omega_{wi} \leq \omega_{\max}, \quad (17)$$

$$|s_i| \leq s_{\max}, \quad (18)$$

where,  $i \in \{F, R\}$  denoting front or rear;  $\omega_{\min}$  and  $\omega_{\max}$  are determined from the efficiency map (Fig. 1).

#### 3) Nonlinear Model Predictive Control:

NMPC works for this RB control problem following three steps.

First, at sampling instant  $k$ , measure the current system states  $\mathbf{x}(k) = [v(k) \ \omega_{wF}(k) \ \omega_{wR}(k)]^T$ . Also, the previous input  $\mathbf{u}(k-1)$  generated by NMPC is kept in memory.

Then, rearrange the control sequence within control horizon  $\{\mathbf{u}(k), \mathbf{u}(k+1), \dots, \mathbf{u}(k+h_c-1)\}$  as

$$\mathbf{U}(k) = [T_{bF}(k) \ \dots \ T_{bF}(k+h_c-1) \ T_{bR}(k) \ \dots \ T_{bR}(k+h_c-1)]^T \quad (19)$$

and solve the nonlinear optimization problem where cost function is defined in (14).

$$\mathbf{U}^*(k) = \min_{\mathbf{U}(k)} J, \quad (20)$$

subjected to nonlinear model (6)~(13) in the prediction horizon and constraints (16)~(18).

Third, the current desirable control input vector is taken to be

$$\mathbf{u}^*(k) = [T_{bF}^*(k) \ T_{bR}^*(k)]^T, \quad (21)$$

and is applied to the system.

Finally, for the next instant, with  $\mathbf{u}^*(k)$  and measured  $\mathbf{x}(k+1)$ , the same procedure is repeated to generate the control input vector  $\mathbf{u}^*(k+1)$ .

It is important to point out that the length of control horizon  $h_c$  determines the dimension of manipulated variable  $\mathbf{U}(k)$  and therefore the size of the optimization problem, while the length of prediction horizon  $h_p$  decides to what extent NMPC can “predict”, thus affecting control performance. In fact, prediction horizon window is typically much smaller than the entire optimization time window, therefore this finite horizon NMPC only provides “semi-optimal” solutions. Furthermore, since  $h_c \leq h_p$ , for simplicity, the control inputs outside of control horizon and inside prediction horizon will take the last value in the control horizon, that is,

$$T_{bi}(k+h_c+j) = T_{bi}(k+h_c-1), \quad j = 0, 1, \dots, h_p - h_c. \quad (22)$$

#### IV. CASE STUDY: OPTIMAL VEHICLE VELOCITY PROFILE

In a typical adaptive cruise control transitional maneuver [10][11], the initial vehicle velocity is known, and the terminal velocity and the desired travelling distance are determined by some higher-level controller. Such constraints on vehicle kinematics give rise to optimal vehicle velocity profile design, in which the main purpose is to gain as much RB energy as possible.

If either one of the two terminal constraints—terminal velocity and total travelling distance is missing, the problem becomes an open-loop optimum seeking problem. In other words, at each time step, for a measured wheel speed, there exists a most energy efficient braking torque value according to the motor-to-battery RB efficiency map (Fig. 1). However,

if the constraints are all exerted and the problem is solvable (which means the required distance is within reachable range), the design of velocity profile may have effects on the amount of RB energy that can be recovered. Moreover, the involvements of environmental disturbances, such as road slope and wind force, can make the problem even more complicated.

This case study aims to provide insight into the effects that different velocity profiles can have on the RB energy recovery, rather than design the optimal profile. An intuitive indication from the efficiency map in Fig. 1 is that the larger wheel speed and braking torque, the higher RB efficiency. This suggests that one efficient RB strategy is to apply large braking torque at the beginning stage of deceleration, where velocity is high, and then after velocity has reached some lower level, apply small or even zero braking torque in order to satisfy the terminal constraints. On the contrary, if small braking torque is first applied followed by large braking torque, the recovered RB energy may not be as much as that in the previous case though terminal constraints are still satisfied.

Once the vehicle velocity profile is somehow determined, the NMPC scheme developed in the previous section can be used for the torque distribution. It is important to point out that wheel dynamics should be taken into account when designing globally optimal velocity profile. Nevertheless, 3-DOF dynamic model renders the problem too complicated and cannot be isolated from the previous problem. Hence, for simplicity, only one manipulated input, the total braking torque, is considered in designing velocity profile. As a result, the design of such a semi-optimal velocity profile may also apply a higher-level NMPC control algorithm, which together with the lower-level NMPC developed in the previous section, constitutes a two-level NMPC-based RB controller for the EVs with in-wheel motors.

The dynamic equations for the higher-level controller are shown below.

$$\dot{d} = v, \quad d(0) = 0, d(t_f) = d_f, \quad (23)$$

$$m\dot{v} = T_b/r_e - F_f - F_a, \quad v(0) = v_0, v(t_f) = v_f, \quad (24)$$

where,  $d$  is the distance vehicle travels,  $T_b$  is the total braking torque,  $F_f$  is the rolling resistance force. The problem can therefore be transferred from velocity profile design to seeking the optimal  $T_b$  as a function of time. To incorporate RB efficiency map, the following approximation is needed.

$$\omega = v/r_e. \quad (25)$$

Simulation results under different velocity profiles are given in the following section.

#### V. SIMULATION RESULTS AND ANALYSES

For the first problem, comparisons were made between the proposed NMPC and a conventional PI controller. A full-vehicle model provided by CarSim<sup>®</sup> was used in the simulations.

### A. Simulation Results of Velocity Tracking Problem

Parameter values used in simulations are listed in Table I.

TABLE I  
PARAMETERS IN VELOCITY TRACKING PROBLEM

Parameter	Value	Unit
$m$	300	kg
$J$	1.9	kg.m <sup>2</sup>
$r_e$	0.33	m
$\gamma$	0.01	-
$h$	0.43	m
$h_a$	0.43	m
$l_F$	1.09	m
$l_R$	0.8	m
$C_a$	0.037	Ns <sup>2</sup> /m <sup>2</sup>
$k_x$	10.2	-
$s_{\max}$	0.03	-
$h_p$	10	-
$h_c$	4	-
$w_r$	1	-
$w_u$	0.0001	-

As can be seen, the simulation is based on a small-scaled vehicle mainly for the purpose of expanding the deceleration range with limited motor capability. As a comparison, the PI controller determines the total braking torque and distributes it to front and rear wheels according to normal forces in real time, that is

$$\frac{T_{bF,PI}}{T_{bR,PI}} = \frac{F_{zF}}{F_{zR}}. \quad (26)$$

The proportional and integral gains for the PI controller are tuned by trial-and-error. A too small gain leads to an unsatisfactory tracking performance, while a too large gain may result in oscillations or even instability. Desired velocity trajectory can be expressed as a function of time.

$$v_f = 24 - 1.5t - \sin(0.4\pi t). \quad (27)$$

The total recovered RB energy and velocity tracking performance are shown in Fig. 3. Braking torque evolutions of both controllers are demonstrated in Fig. 4.

As can be seen, the energy recovered using the proposed NMPC is more than that of using a PI controller, while the vehicle tracking performance is almost same. From the braking torque curve, it is easily seen that distributing the total braking torque according to (26) is not an energy-efficient way, especially when the braking torque is small. In fact, around 2 or 7 second, NMPC applies almost all braking torque to front wheels. This can be explained by the unique shape on the RB efficiency map where braking torque is low. On the contrary, the PI controller always applies slightly larger braking torque on rear wheels due to larger normal loads. Another observation is that the hard constraint (16) on braking torque is reached for NMPC at the beginning of the simulation due to high deceleration demand.

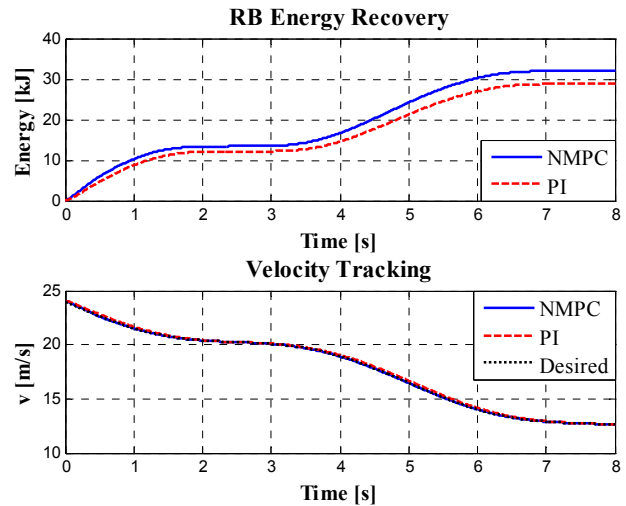


Fig. 3. Comparisons of Energy Recovery and Velocity Tracking

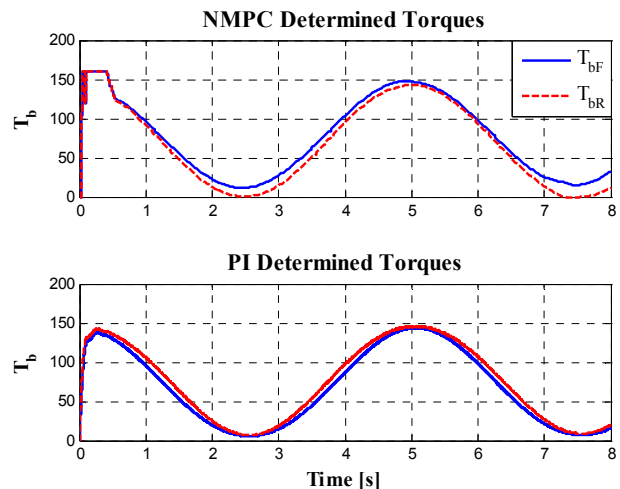


Fig. 4. Braking Torques of Using NMPC and PI Controller

### B. Simulation for Velocity Profile Planning

To show the effects of velocity profile on RB energy recovery, four different velocity profiles with the same initial and terminal velocities, 24 m/s and 9 m/s, as well as a total distance, 165m are designed, as shown in Fig. 5. Brief descriptions of these profiles and the RB energy recovered for them are listed in Table II.

As can be observed and deduced from the figure and table, due to the existence of strict terminal constraints, the duration of the entire deceleration is free of change. For some traffic control problems, this duration may also be subjected to constraint. Among all velocity profiles, the “harsh-gentle” braking pattern is the most efficient way, which matches with the previous discussion, while the “gentle-harsh” pattern recovers the least RB energy. This result provides a rule-of-thumb in designing energy-efficient velocity profiles.

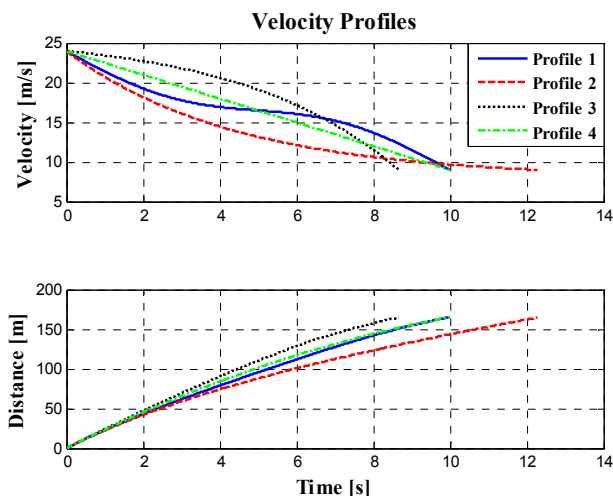


Fig. 5. Different Velocity and Distance Profiles.

TABLE II  
RECOVERED RB ENERGY UNDER DIFFERENT VELOCITY PROFILE

	Profile 1	Profile 2	Profile 3	Profile 4
Profile Description	Sinusoidal	Harsh-Gentle	Gentle-Harsh	Constant Deceleration
RB Energy (kJ)	33.59	35.20	30.89	32.23

## VI. CONCLUSIONS AND FUTURE WORK

In this paper, a NMPC-based RB controller is developed for energy recovery during regenerative braking for EVs with in-wheel motors. Simulation results show that for velocity track problem, NMPC is able to recover more RB energy than a traditional PI controller by wisely distributing braking torque to the front and rear wheels without scarification of vehicle velocity tracking performance. A case study is also provided for fixed terminal velocity and distance problem and shows great potentials in using NMPC to achieve RB energy improvement by designing a semi-optimal velocity profile.

Though satisfactory at this preliminary stage, the proposed NMPC method can still be improved in the following aspects: 1) The proposed NMPC can be made adaptive to model uncertainties, for example, slip slope  $k_x$ , which is an unknown constant in most cases; 2) some techniques are needed in speeding up the computation process; 3) NMPC for RB energy recovery can be extended to some more complex maneuvers, such as braking when cornering.

## REFERENCES

- [1] P. Falcone, S. Khoshfetrat Pakazad and S. Solyom, "Predictive approaches to rear axle regenerative braking control in hybrid vehicles", in *Decision and Control, 2009 held jointly with the 2009 28th Chinese Control Conference. CDC/CCC 2009. Proceedings of the 48th IEEE Conference on*, 2009, pp. 7627-7632.
- [2] P. Kokotovic and G. Singh, "Minimum-energy control of a traction motor", *Automatic Control, IEEE Transactions on*, vol. 17, no. 1, pp. 92-95, 1972.
- [3] J. Guo, J. Wang and B. Cao, "Regenerative Braking Strategy for Electric Vehicles", *IEEE Intelligent Vehicles Symposium*, pp. 864-868, 2009.

- [4] J. Zhang, B. Song and X. Niu, "Optimization of Parallel Regenerative Braking Control Strategy", *IEEE Vehicle Power and Propulsion Conference (VPPC)*, Harbin, China, Sept. 2008.
- [5] P. Suntharalingam, J. T. Economou and K. Knowles, "Effect on Regenerative Braking Efficiency with Deceleration Demand and Terrain Condition", *5th IET International Conference on Power Electronics, Machines and Drives*, 2010.
- [6] J. Cao, et al., "Neural Network Self-adaptive PID Control for Driving and Regenerative Braking of Electric Vehicle", *IEEE International Conference on Automation and Logistics*, Jinan, China, Aug. 2007.
- [7] J. Cao, et al., "Regenerative-Braking Sliding Mode Control of Electric Vehicle Based on Neural Network Identification", *IEEE/ASME International Conference on Advanced Intelligent Mechatronics*, Xi'an, China, July 2008.
- [8] Z. Zhang, et al., "Regenerative Braking for Electric Vehicle based on Fuzzy Logic Control Strategy", *2nd International Conference on Mechanical and Electronics Engineering*, vol. 1, pp. 319-323, 2010.
- [9] J. Xie, et al., "Switched Robust Control of Regenerative Braking of Electric Vehicles", *IEEE International Conference on Information and Automation*, Harbin, China, June 2010.
- [10] B. Asadi and A. Vahidi, "Predictive Cruise Control: Utilizing Upcoming Traffic Signal Information for Improving Fuel Economy and Reducing Trip Time", *Control Systems Technology, IEEE Transactions on*, vol. 19, no. 3, pp. 707-714, 2011.
- [11] V. L. Bageshwar, et al., "Model predictive control of transitional maneuvers for adaptive cruise control vehicles", *Vehicular Technology, IEEE Transactions on*, vol. 53, no. 5, pp. 1573-1585, 2004.
- [12] R. Wang, Y. Chen, D. Feng, X. Huang, and J. Wang, "Development and Performance Characterization of an Electric Ground Vehicle with Independently-Actuated In-Wheel Motors", *Journal of Power Sources*, vol. 196, no. 8, pp. 3962 - 3971, 2011.
- [13] M. Hsieh, J. Wang, and M. Canova, "Two-Level Nonlinear Model Predictive Control for Lean NO<sub>x</sub> Trap Regenerations", *Journal of Dynamic Systems, Measurement, and Control*, vol. 132, no. 4, 041001 (13 pages), 2010.
- [14] M. Canale, L. Fagiano and V. Razza, "Approximate NMPC for vehicle stability: Design, implementation and SIL testing", *Control Engineering Practice*, vol. 18, no. 6, pp. 630-639, 2010.
- [15] Luigi del Re et al., *Automotive Model Predictive Control: Models, Methods and Applications*, Springer, 2010.
- [16] S. Joe Qin and T. A. Badgwell, "A survey of industrial model predictive control technology", *Control Engineering Practice*, vol. 11, no. 7, pp. 733-764, 2003.
- [17] D. Q. Mayne, et al., "Constrained model predictive control: Stability and optimality", *Automatica*, vol. 36, no. 6, pp. 789-814, 2000.
- [18] J. Wang, L. Alexander and R. Rajamani, "Friction estimation on highway vehicles using longitudinal measurements", *Journal of Dynamic Systems, Measurement, and Control*, vol. 126, no. 2, pp. 265-275, 2004.
- [19] R. Rajamani et al., "Tire-road Friction-Coefficient Estimation", *IEEE Control Systems Magazine*, vol. 30, no. 4, pp. 54-69, 2010.
- [20] Y. Chen and J. Wang, "Fast and Global Optimal Energy-Efficient Control Allocation with Applications to Over-Actuated Electric Ground Vehicles," *IEEE Transactions on Control Systems Technology* (in press), 2011.
- [21] Y. Chen and J. Wang, "Adaptive Vehicle Speed Control with Input Injections for Longitudinal Motion Independent Road Frictional Condition Estimation," *IEEE Transactions on Vehicular Technology*, Vol. 60, No. 3, pp. 839 - 848, 2011.